3D Path Following for Autonomous Underwater Vehicle[1]

P. Encarnação A. Pascoal

Institute for Systems and Robotics and Dept. Electrical Eng.
Instituto Superior Técnico
Av. Rovisco Pais, 1, 1049-001 Lisboa, Portugal
E-mail:{pme,antonio}@isr.ist.utl.pt

Abstract

A new methodology is proposed for the design of path following systems for autonomous underwater vehicles. Global convergence to reference paths is achieved with a nonlinear control strategy that takes explicitly into account the dynamics of the vehicle. Formal convergence proofs are indicated. Simulation results with the model of a prototype autonomous underwater vehicle are presented to illustrate the performance of the path following system derived.

1 Introduction

This paper proposes a new methodology for the design of path following systems for autonomous underwater vehicles. This problem has been motivated by the practical need to develop such a control system for INFANTE, an autonomous underwater vehicle (AUV) developed at the Instituto Superior Técnico (Pascoal *et al.*, 2000). The reader is referred to (Samson, 1992; Micaelli and Samson, 1993) and the references therein for related work in the field of land robots, where methods for path following have been devised that rely on Lyapunov-based nonlinear control. The techniques proposed essentially solve the problem of path following for land vehicles by taking into account the kinematic equations only. However, they cannot be simply extended to air or underwater vehicles. In this case, new methodologies for path following are required to take explicitly into account the presence of complex aero/hydrodynamic terms in the vehicle dynamics.

The work reported in (Micaelli and Samson, 1993) has recently been extended for the case of marine craft in the presence of constant but unknown ocean currents. In (Encarnação *et al.*, 2000) the authors describe a nonlinear path following control system that takes explicitly into account the dynamics of the vehicle as well as those of a current estimator. The same circle of ideas is explored here for the three dimensional case. The envisioned applications are AUVs that are only actuated in surge, pitch, and yaw. Thus, the system is not feedback linearizable and other nonlinear control approaches must be sought.

[1]This work was supported in part by the Commission of the European Communities under contract no. MAS3-CT97-0092, (ASIMOV) and the Portuguese PRAXIS programme under projects INFANTE and CARAVELA. The first author benefited from a PRAXIS XXI Graduate Fellowship.

The key ideas behind the development of the nonlinear control strategy can be simply explained as follows. An hypothetical vehicle is considered that has its main body axis aligned with the total velocity vector and a nonlinear "kinematic" controller is derived for that vehicle to steer it to a reference path. Asymptotic convergence to the reference path is proven for this control system. Then, the "kinematic" controller derived is extended to incorporate the dynamics. This is done by casting the vehicle dynamic equations into standard integrator form using nonlinear dynamic inversion (Isidori, 1989) and applying backstepping techniques (Krstić *et al.*, 1995). It is assumed that the position and attitude of the underwater vehicle, as well as its angles of attack and sideslip, are accessible for measurement. Formal convergence proofs are indicated. Simulation results with the model of a prototype autonomous underwater vehicle are presented to illustrate the performance of the resulting path following controller.

An introduction to the problem of path following for air and underwater vehicles can be found in (Kaminer *et al.*, 1998), (Fryxell *et al.*, 1996), where the authors proposed the use of gain scheduled techniques for accurate vehicle control about trimming paths. Stability and performance results were thus only local in nature. The reader will find in (Krstić *et al.*, 1995) a lucid presentation of backstepping techniques. See also (Fossen and Berge, 1997; Aamo *et al.*, 2000) for interesting applications to ship control.

2 Kinematic and dynamic model of an AUV. The path following problem.

This section derives the dynamic model of an AUV and introduces the path following problem. See (Fryxell, 1994; Silvestre and Pascoal, 1997) for details on the construction, modelling, and control of a representative AUV prototype.

Following standard practice, the equations of motion of an AUV can be developed using a global coordinate frame $\{U\}$ and a body-fixed coordinate frame $\{B\}$ that moves with the vehicle. The following notation is required (Fryxell, 1994; Silvestre and Pascoal, 1997): ${}^{B}v_{B_{org}} \equiv (u, v, w)^T$ is the velocity of the origin of $\{B\}$ relative to $\{U\}$, expressed in $\{B\}$ (i.e., body-fixed linear velocity) and ${}^{B}\omega_{B} \equiv (p, q, r)^T$ is the angular velocity of $\{B\}$ relative to $\{U\}$, expressed in $\{B\}$ (i.e., body-fixed angular velocity). From Newton-Euler equations,

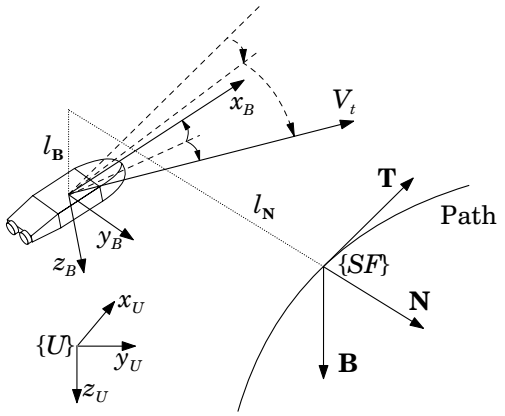

Figure 1: Vehicle following a 3D path.

the translational and rotational motion of the AUV are described by

$$\begin{aligned} X+T &= m\left(\dot{u}+qw-rv\right) \\ Y &= m\left(\dot{v}+ru-pw\right) \\ Z &= m\left(\dot{w}+pv-qu\right) \\ K &= I_x\dot{p}+\left(I_z-I_y\right)qr \\ M &= I_y\dot{q}+\left(I_x-I_z\right)pr \\ N &= I_z\dot{r}+\left(I_y-I_x\right)pq \end{aligned}$$

where (X, Y, Z) are the forces along the body-fixed frame $\{B\}$, (K, M, N) are the rolling, pitching and yawing moments about frame $\{B\}$, and I_x, I_y, and I_z are the moments of inertia about the same frame. In the equations, T is the thrust force along the x_B axis that is generated by the back propellers, and m is the vehicle mass. The external forces and moments include (restoring) terms caused by gravity and buoyancy, added mass terms, the effects of control surface deflections, and centripetal, Coriolis, and friction as well as hydrodynamic damping forces and moments acting on the vehicle's body. In what follows it is convenient to express the translational motion of the vehicle in terms of its total linear speed V_t, angle of attack α, and sideslip angle β, which are related to u, v, and w as

$$\begin{aligned} V_t &= \sqrt{u^2+v^2+w^2}, \\ \alpha &= \arctan\left(\tfrac{w}{u}\right), \\ \beta &= \arcsin\left(\tfrac{v}{V_t}\right), \end{aligned}$$

respectively. A simplified model for the external forces and moments is given by (Fryxell, 1994; Fossen, 1994)

$$\begin{aligned} X &= \tfrac{1}{2}\rho V_t^2L^2\left(X_{uu}+X_{vv}\beta^2\right) \\ Y &= \tfrac{1}{2}\rho V_t^2L^2\left(Y_v\beta+Y_r\tfrac{rL}{V_t}\right) \\ Z &= \tfrac{1}{2}\rho V_t^2L^2\left(Z_w\alpha+Z_q\tfrac{qL}{V_t}\right) \\ K &= \tfrac{1}{2}\rho V_t^2L^3K_p\tfrac{pL}{V_t}+z_{CB}\cos\theta'\sin\phi'\rho g\overline{V} \\ M &= \tfrac{1}{2}\rho V_t^2L^3\left(M_w\alpha+M_q\tfrac{qL}{V_t}+M_{\delta_b}\delta_b+M_{\delta_s}\delta_s\right) \\ &\quad +z_{CB}\sin\theta'\rho g\overline{V} \\ N &= \tfrac{1}{2}\rho V_t^2L^3\left(N_v\beta+N_r\tfrac{rL}{V_t}+N_{\delta_r}\delta_r\right) \end{aligned}$$

where ρ is the fluid density, L is a representative vehicle length, and $X_{(\cdot)}$, $Y_{(\cdot)}$, $Z_{(\cdot)}$, $K_{(\cdot)}$, $M_{(\cdot)}$, and $N_{(\cdot)}$ are hydrodynamic coefficients. In addition, z_{CB} is the metacentric hight, $\overline{V}$ is the vehicle's volume, g is the gravity acceleration, θ' and ϕ' are the pitch and yaw angles from the body fixed to the global frame, and δ_b, δ_s, and δ_r are the bow and stern plane and the rudder deflections, respectively. In this work, it was assumed that the vehicle is neutrally buoyant. Pure forces due to the deflection of the control surfaces, as well as added mass and higher order hydrodynamical terms were neglected.

Assuming the vehicle's speed is held constant, the V_t equation is discarded and the vehicle dynamic model can be written as (1)-(5).

This paper addresses the problem of designing a feedback controller for an underwater vehicle with dynamics described by (1)-(5) to drive it along a desired path with constant speed. Intuitively, the path following controller should look at i) the distance from the vehicle to the path and ii) the angles between the vehicle velocity and the tangent to the path, and reduce both to zero (Samson, 1992; Micaelli and Samson, 1993). This motivates the development of the vehicle kinematic model in terms of so-called Serret-Frenet frame and the use of the above distance and angles as coordinates of the error space where the control problem will be formulated. The following additional notation is required.

Let $\{W\}$ be the frame that results from $\{B\}$ by rotating it about y_B through the angle of attack α, followed by a rotation about z_B through the sideslip angle β. Thus, $\{W\}$ has its x_W axis aligned with the total velocity vector; following standard nomenclature in aircraft control, $\{W\}$ will be called the "wind" frame. The symbol ${}^{W}R_B\left(\alpha,\beta\right)$ denotes the rotation matrix from $\{B\}$ to $\{W\}$, parameterized by α and β. Consider also $\{SF\}$, the Serret-Frenet frame associated with each point of the path, with unity vectors $\mathbf{T}$ (tangent to the path), $\mathbf{N}$ (normal to the path), and $\mathbf{B}=\mathbf{T}\times\mathbf{N}$. Let s be the distance along the path, k the path's curvature, and τ its torsion. The path's curvature k and torsion τ are assumed to be continuous bounded functions of s with bounded derivatives but, for simplicity of notation, their dependence on s is not written down explicitly. According to the well-known Serret-Frenet formulas, the angular velocity of $\{SF\}$ measured in $\{U\}$ and expressed in $\{SF\}$ is given by ${}^{SF}\omega_{SF}=\left(\tau\dot{s},0,k\dot{s}\right)^T$. Let $l_{\mathbf{N}}$ and $l_{\mathbf{B}}$ denote the signed distances between the vehicle center of mass and the origin of the Serret-Frenet frame (at the point on the path that is closest to the vehicle) along the $\mathbf{N}$ and $\mathbf{B}$ axes respectively, i.e., ${}^{SF}P_{org_W}=\left(0,l_{\mathbf{N}},l_{\mathbf{B}}\right)^T$. With this notation, the relative velocity between the wind and the Serret-Frenet frames is $\frac{d\,{}^{SF}P_{org_W}}{dt}=\left(0,\dot{l}_{\mathbf{N}},\dot{l}_{\mathbf{B}}\right)^T$. Let ${}^{SF}R_W\left(\phi,\theta,\psi\right)$ be the rotation matrix from the Serret-Frenet frame to the wind frame that is parameterized locally by the roll (ϕ), pitch (θ), and yaw (ψ) angles. Propagating the vehicle linear velocities from the wind frame to the Serret-Frenet frame yields (Craig, 1986)

$${}^{SF}R_W\left(\phi,\theta,\psi\right){}^{W}v_B = {}^{SF}v_{SF}+\tfrac{d\,{}^{SF}P_{org_W}}{dt}+ {}^{SF}\omega_{SF}\times{}^{SF}P_{org_W} \qquad (6)$$

where ${}^{W}v_B=\left(V_t,0,0\right)^T$ is the vehicle linear velocity

$$\dot{\alpha} = -\cos\alpha\tan\beta p + \left(1 + \frac{\rho L^3}{2m\cos\alpha\cos\beta} Z_q\right) q + \left(-\sin\alpha\tan\beta + \frac{\rho L^3 \tan\alpha\tan\beta}{2m\cos\beta} Y_r\right) r + \frac{\rho V_t L^2 \tan\alpha\tan\beta}{2m\cos\beta} Y_v\beta + \frac{\rho V_t L^2}{2m\cos\alpha\cos\beta} Z_w\alpha \quad (1)$$

$$\dot{\beta} = \sin\alpha p + \left(-\cos\alpha + \frac{\rho L^3}{2m\cos\beta} Y_r\right) r + \frac{\rho V_t L^2}{2m\cos\beta} Y_v\beta \quad (2)$$

$$\dot{p} = -\frac{I_z - I_y}{I_x} qr + \frac{1}{I_x}\left(\frac{1}{2}\rho V_t^2 L^3 K_p \frac{pL}{V_t} + z_{CB}\cos\theta'\sin\phi'\rho g\overline{V}\right) \quad (3)$$

$$\dot{q} = -\frac{I_x - I_z}{I_y} pr + \frac{1}{I_y}\left(\frac{1}{2}\rho V_t^2 L^3 \left(M_w\alpha + M_q\frac{qL}{V_t} + M_{\delta_b}\delta_b + M_{\delta_s}\delta_s\right) + z_{CB}\sin\theta'\rho g\overline{V}\right) \quad (4)$$

$$\dot{r} = -\frac{I_y - I_x}{I_z} pq + \frac{1}{I_z}\left(\frac{1}{2}\rho V_t^2 L^3 \left(N_v\beta + N_r\frac{rL}{V_t} + N_{\delta_r}\delta_r\right)\right). \quad (5)$$

---

measured in $\{U\}$ and expressed in $\{W\}$ and ${}^{SF}v_{SF} = (\dot{s}, 0, 0)^T$ is the Serret-Frenet frame linear velocity measured in $\{U\}$ and expressed in $\{SF\}$. Expanding (6) gives

$$\begin{aligned} \dot{s} &= \frac{V_t\cos\theta\cos\psi}{1 - l_{\mathbf{N}}k} \\ \dot{l}_{\mathbf{N}} &= V_t\cos\theta\sin\psi + l_B\tau\dot{s} \\ \dot{l}_{\mathbf{B}} &= -V_t\sin\theta - l_{\mathbf{N}}\tau\dot{s}. \end{aligned}$$

To derive the equations for the evolution of ϕ, θ, and ψ, one can compute the wind frame angular velocity relative to the Serret-Frenet frame $\left({}^{W}\omega^{r}_{W,SF}\right)$ as the difference between the angular velocity ${}^{W}\omega_{W}$ of $\{W\}$ and the angular velocity ${}^{W}\omega_{SF}$ of $\{SF\}$. Since ${}^{W}\omega_{W}$ is the sum of the angular velocity ${}^{W}\omega^{r}_{W,B}$ of $\{W\}$ relative to $\{B\}$ with the angular velocity ${}^{W}\omega_{B}$ of $\{B\}$, it follows that

$${}^{W}\omega^{r}_{W,SF} = {}^{W}\omega^{r}_{W,B} + {}^{W}\omega_{B} - {}^{W}\omega_{SF},$$

where

$$\begin{aligned} {}^{W}\omega^{r}_{W,B} &= \begin{bmatrix} 0 \\ 0 \\ \dot{\beta} \end{bmatrix} + \begin{bmatrix} \cos\beta & \sin\beta & 0 \\ -\sin\beta & \cos\beta & 0 \\ 0 & 0 & 1 \end{bmatrix} \begin{bmatrix} 0 \\ -\dot{\alpha} \\ 0 \end{bmatrix}, \\ {}^{W}\omega_{B} &= {}^{W}R_{B}(\alpha,\beta)\ {}^{B}\omega_{B}, \\ {}^{W}\omega_{SF} &= {}^{W}R_{SF}(\phi,\theta,\psi)\ {}^{SF}\omega_{SF}. \end{aligned}$$

Now, the derivatives of the roll, pitch and yaw angles can be computed using the Jacobian operator that relates the angular velocity of $\{W\}$ with the angular rates (Craig, 1986). Performing all the computations described and using (1) and (2) yields the "kinematic" model for the velocity vector (7)-(12).[1]

$$\dot{s} = \frac{V_t c\theta c\psi}{1 - l_{\mathbf{N}}k} \quad (7)$$

$$\dot{l}_{\mathbf{N}} = V_t c\theta s\psi + l_B\tau\dot{s} \quad (8)$$

$$\dot{l}_{\mathbf{B}} = -V_t s\theta - l_{\mathbf{N}}\tau\dot{s} \quad (9)$$

[1] The symbols $s(\cdot)$, $c(\cdot)$, and $t(\cdot)$ denote the trigonometric functions $\sin(\cdot)$, $\cos(\cdot)$, and $\tan(\cdot)$, respectively.

3 Kinematic control design

To drive the vehicle to a reference geometric path, it is necessary to align the total velocity vector with the tangent to the path $\mathbf{T}$. When those vectors are aligned, possible errors in roll do not affect path following and should not be compensated. Moreover, in the AUV model there is no direct control over the angular velocity p. Therefore, the goal of the kinematic controller is to drive the distances $l_{\mathbf{N}}$ and $l_{\mathbf{B}}$, as well as the angular displacements θ and ψ to zero. To do this, the kinematic controller uses the angular velocities q and r.

From (11) and (12) it follows that the subsystem formed by θ and ψ has vector relative degree $(1,1)$. Thus, a feedback linearization control law can be used to linearize the equations; namely, setting

$$\begin{bmatrix} q \\ r \end{bmatrix} = D_1^{-1}\left(-E_1 + \begin{bmatrix} \upsilon_q \\ \upsilon_r \end{bmatrix}\right), \quad (13)$$

where D_1 and E_1 are easily obtained by inspection of (11) and (12), gives

$$\dot{\theta} = \upsilon_q + s\psi\tau\dot{s} \quad (14)$$

$$\dot{\psi} = \upsilon_r - t\theta c\psi\tau\dot{s} - k\dot{s}. \quad (15)$$

In order to have some control over the transient properties of the control system, it is important to shape the evolution of the vehicle trajectory as it approaches the desired path. This motivates the choice of the Lyapunov function candidate

$$V_1 = \frac{1}{2}\left(l_{\mathbf{B}}^2 + l_{\mathbf{N}}^2 + a(\theta - f(l_{\mathbf{B}}))^2 + b(\psi - g(l_{\mathbf{N}}))^2\right)$$

for kinematic control analysis and design, where $f(l_{\mathbf{B}})$ and $g(l_{\mathbf{N}})$ are nonlinear functions that impose transient behaviours for θ and ψ, respectively. Following (Micaelli and Samson, 1993), $f(l_{\mathbf{B}})$ can be chosen such that $\lim_{l_{\mathbf{B}}\to\infty} f(l_{\mathbf{B}}) = \theta_d$ and $\lim_{l_{\mathbf{B}}\to 0} f(l_{\mathbf{B}}) = 0$, where θ_d is a design parameter. Intuitively, the function $f(l_{\mathbf{B}})$ saturates to a value θ_d when the vehicle is away from the path. Similar comments apply to $g(l_{\mathbf{N}})$. Some

$$\dot{\phi} = \frac{c\alpha}{c\beta}p + \left(-\frac{\rho L^3 t\beta}{2mc\alpha}Z_q - \frac{\rho L^3 s\phi t\theta}{2mc\alpha}Z_q\right)q + \left(\frac{s\alpha}{c\beta} - \frac{\rho L^3 t\alpha\,(t\beta)^2}{2m}Y_r - \frac{\rho L^3 s\phi t\theta t\alpha t\beta}{2m}Y_r + \frac{\rho L^3 c\phi t\theta}{2mc\beta}Y_r\right)r +$$
$$\left(-\frac{\rho V_t L^2 t\alpha\,(t\beta)^2}{2m}Y_v\beta - \frac{\rho V_t L^2 t\beta}{2mc\alpha}Z_w\alpha - \frac{\rho V_t L^2 s\phi t\theta t\alpha t\beta}{2m}Y_v\beta - \frac{\rho V_t L^2 s\phi t\theta}{2mc\alpha}Z_w\alpha + \frac{\rho V_t L^2 c\phi t\theta}{2mc\beta}Y_v\beta\right) - \frac{c\psi}{c\theta}\tau\dot{s} \quad (10)$$

$$\dot{\theta} = \left(-\frac{\rho L^3 c\phi}{2mc\alpha}Z_q\right)q + \left(-\frac{\rho L^3 c\phi t\alpha t\beta}{2m}Y_r - \frac{\rho L^3 s\phi}{2mc\beta}Y_r\right)r +$$
$$\left(-\frac{\rho V_t L^2 c\phi t\alpha t\beta}{2m}Y_v\beta - \frac{\rho V_t L^2 c\phi}{2mc\alpha}Z_w\alpha - \frac{\rho V_t L^2 s\phi}{2mc\beta}Y_v\beta\right) + s\psi\tau\dot{s} \quad (11)$$

$$\dot{\psi} = \left(-\frac{\rho L^3 s\phi}{2mc\theta c\beta}Z_q\right)q + \left(-\frac{\rho L^3 s\phi t\alpha t\beta}{2mc\theta}Y_r + \frac{\rho L^3 c\phi}{2mc\theta c\beta}Y_r\right)r +$$
$$\left(-\frac{\rho V_t L^2 s\phi t\alpha t\beta}{2mc\theta}Y_v\beta - \frac{\rho V_t L^2 s\phi}{2mc\theta c\alpha}Z_w\alpha + \frac{\rho V_t L^2 c\phi}{2mc\theta c\beta}Y_v\beta\right) - t\theta c\psi\tau\dot{s} - k\dot{s}. \quad (12)$$

restrictions to these functions can be found in Theorem 1. The positive constants a and b are instrumental in balancing the competing goals of driving the position and orientation errors to zero and are additional design parameters to shape closed loop vehicle behaviour. The main result of this section follows.

Theorem 1 *Consider the closed loop system consisting of (7)-(10),(14)-(15) and the control law*

$$\begin{aligned} v_q &= \tfrac{l_{\mathbf{B}}}{a}V_t\tfrac{\sin\theta-\sin f}{\theta-f} - \tau\sin\psi\dot{s} - f'_{l_{\mathbf{B}}}V_t\sin\theta \\ &\quad -f'_{l_{\mathbf{B}}}l_{\mathbf{N}}\tau\dot{s} - k_\theta\,(\theta-f) \text{ and} \\ v_r &= -\tfrac{l_{\mathbf{N}}V_t\cos\theta}{b}\tfrac{\sin\psi-\sin g}{\psi-g} + \tau\cos\psi\tan\theta\dot{s} + k\dot{s} \\ &\quad +g'_{l_{\mathbf{N}}}V_t\sin\psi\cos\theta + g'_{l_{\mathbf{N}}}l_{\mathbf{B}}\tau\dot{s} - k_\psi\cos\theta\,(\psi-g) \end{aligned} \quad (16)$$

where $k_\theta, k_\psi > 0$, $f, g : \Re\times\Re\to\Re$ are C^1 functions, $f'_{l_{\mathbf{B}}}$ is the derivative of f with respect to $l_{\mathbf{B}}$, and $g'_{l_{\mathbf{N}}}$ is the derivative of g with respect to $l_{\mathbf{N}}$. If hypothesis

H1: $f(0) = g(0) = 0$,

H2: $|f(l_{\mathbf{B}})| < \frac{\pi}{2}, \forall_{l_{\mathbf{B}}}$,

H3: $|g(l_{\mathbf{N}})| < \frac{\pi}{2}, \forall_{l_{\mathbf{N}}}$,

H4: $l_{\mathbf{B}}u\sin f(l_{\mathbf{B}}) \geq 0, \forall_{l_{\mathbf{B}}}$,

H5: $l_{\mathbf{N}}u\sin g(l_{\mathbf{N}}) \leq 0, \forall_{l_{\mathbf{N}}}$,

hold, $l_{\mathbf{N}} \neq 1/k$, and α, β, and θ remain within $-\frac{\pi}{2}$ and $\frac{\pi}{2}$, then $l_{\mathbf{N}}$, $l_{\mathbf{B}}$, θ, and ψ converge to zero.

Proof: Consider the partial Lyapunov function candidate

$$V_1 = \frac{1}{2}\left(l_{\mathbf{B}}^2 + l_{\mathbf{N}}^2 + a\,(\theta - f\,(l_{\mathbf{B}}))^2 + b\,(\psi - g\,(l_{\mathbf{N}}))^2\right),$$

where a and b are positive scalars and f and g satisfy hipothesis H1 through H5.

The time derivative of V along the closed loop system trajectories can be easily computed to yield

$$\begin{aligned} \dot{V}_1 &= a\,(\theta-f)\left(v_q + \tau\sin\psi\dot{s} + f'_{l_{\mathbf{B}}}V_t\sin\theta + f'_{l_{\mathbf{B}}}l_{\mathbf{N}}\tau\dot{s}\right) + \\ &\quad b\,(\psi-g)\,(v_r - \tau\cos\psi\tan\theta\dot{s} - k\dot{s} - \\ &\quad g'_{l_{\mathbf{N}}}V_t\sin\psi\cos\theta - g'_{l_{\mathbf{N}}}l_{\mathbf{B}}\tau\dot{s}) - \\ &\quad l_{\mathbf{B}}V_t\sin\theta + l_{\mathbf{N}}V_t\sin\psi\cos\theta. \end{aligned}$$

Adding and subtracting $l_{\mathbf{B}}V_t\sin f$ and $l_{\mathbf{N}}V_t\sin g\cos\theta$, and using (16) gives

$$\begin{aligned} \dot{V}_1 &= -l_{\mathbf{B}}V_t\sin f + l_{\mathbf{N}}V_t\sin g\cos\theta - ak_\theta\,(\theta-f)^2 - \\ &\quad bk_\psi\,(\psi-g)^2, \end{aligned}$$

which, by hypothesis H4 and H5, is negative semidefinite. Now, using Barbalat's lemma, it can be concluded that $l_{\mathbf{N}}$, $l_{\mathbf{B}}$, θ, and ψ converge to zero. ■

As suggested in (Micaelli and Samson, 1993), possible choices for f and g are the sigmoid functions

$$\begin{aligned} f\,(l_{\mathbf{B}}) &= sign(V_t)\theta_d\tfrac{e^{2k_f l_{\mathbf{B}}}-1}{e^{2k_f l_{\mathbf{B}}}+1} \text{ and} \\ g\,(l_{\mathbf{N}}) &= -sign(V_t)\psi_d\tfrac{e^{2k_g l_{\mathbf{N}}}-1}{e^{2k_g l_{\mathbf{N}}}+1}, \end{aligned}$$

where $k_f, k_g > 0$, $0 \leq \theta_d < \frac{\pi}{2}$, $0 \leq \psi_d < \frac{\pi}{2}$, and $sign(\cdot)$ is the signal function. It is straight-forward to verify that these functions satisfy hypothesis H1 to H5.

4 Backstepping kinematics into dynamics

The kinematic controller was designed assuming that the angular velocities q and r were the actual control signals. However, the real vehicle is actuated via control surface deflections. In this section, a backstepping technique (Krstić *et al.*, 1995) is used to modify the kinematic controller to accommodate the vehicle dynamics.

To cast the system in standard integrator backstepping form, it is necessary to compute the derivatives of v_q and v_r. As the vehicle has three sets of control surfaces (bow and stern diving planes and rudders), the equations for $\dot{v}_q$ and $\dot{v}_r$ involve three control inputs, thus preventing the use of a nonlinear inversion technique. In this work, the approach is to consider a single equivalent diving

plane. To do this, the term $M_{\delta_b}\delta_b + M_{\delta_s}\delta_s$ in the moment M is replaced by $M_{\delta_{eq}}\delta_{eq}$, where $M_{\delta_{eq}} = \frac{M_{\delta_b}+M_{\delta_s}}{2}$ is a scale factor that makes δ_{eq} of the same order of magnitude as δ_b and δ_s. Given an equivalent deflection, real control surface deflections are computed in such a way as to make them proportional to the control surface efficiency, as evaluated by the moment coefficients M_{δ_b} and M_{δ_s}. This yields

$$\begin{aligned} \delta_s &= \frac{M_{\delta_s}\left(M_{\delta_b}+M_{\delta_s}\right)}{2M_{\delta_b}^2+2M_{\delta_s}^2}\delta_{eq}, \\ \delta_b &= \frac{M_{\delta_b}}{M_{\delta_s}}\delta_s. \end{aligned}$$

Using this strategy, the derivatives of υ_q and υ_r can be written as

$$\begin{bmatrix} \dot{\upsilon}_q \\ \dot{\upsilon}_r \end{bmatrix} = D_2 \begin{bmatrix} \delta_{eq} \\ \delta_r \end{bmatrix} + E_2, \tag{17}$$

where

$$D_2 = \begin{bmatrix} -\frac{\rho^2 V_t^2 L^6 c\phi}{4mI_y c\alpha} Z_q M_{\delta_{eq}} & -\frac{\rho^2 V_t^2 L^6}{4mI_z}\left(c\phi t\alpha t\beta + \frac{s\phi}{c\beta}\right) Y_r N_{\delta_r} \\ -\frac{\rho^2 V_t^2 L^6 s\phi}{4mI_y c\theta c\alpha} Z_q M_{\delta_{eq}} & -\frac{\rho^2 V_t^2 L^6}{4mI_z}\left(\frac{s\phi t\alpha t\beta}{c\theta} - \frac{c\phi}{c\theta c\beta}\right) Y_r N_{\delta_r} \end{bmatrix}.$$

The expression for E_2 is omitted due to space limitations. It follows that (17) has vector relative degree $(1,1)$. Thus, the input transformation

$$\begin{bmatrix} \delta_{eq} \\ \delta_r \end{bmatrix} = D_2^{-1}\left(-E_2 + \begin{bmatrix} \upsilon_{\delta_{eq}} \\ \upsilon_{\delta_r} \end{bmatrix}\right)$$

leads to the linear decoupled subsystem

$$\begin{bmatrix} \dot{\upsilon}_q \\ \dot{\upsilon}_r \end{bmatrix} = \begin{bmatrix} \upsilon_{\delta_{eq}} \\ \upsilon_{\delta_r} \end{bmatrix}. \tag{18}$$

Let ϕ_q and ϕ_r be the virtual control laws in (16). According to the backstepping method, define $z_q = \upsilon_q - \phi_q$ and $z_r = \upsilon_r - \phi_r$ as the differences between the virtual control variables and the virtual control laws. Intuitively, if z_q and z_r go to zero the system approaches the manifold correspondent to the "kinematic system". This motivates the choice of the Lyapunov function

$$V_2 = V_1 + \frac{1}{2}\left(z_q^2 + z_r^2\right).$$

Differentiating V_2 along the closed loop system trajectories and performing the change of coordinates $\upsilon_q = z_q + \phi_q$ and $\upsilon_r = z_r + \phi_r$ yields

$$\begin{aligned} \dot{V}_2 &= \dot{V}_1 + z_q\left(\upsilon_{\delta_{eq}} - \dot{\phi}_q + a\left(\theta - f\right)\right) + \\ &\quad z_r\left(\upsilon_{\delta_r} - \dot{\phi}_r - b\left(\psi - g\right)\right). \end{aligned}$$

Setting

$$\begin{aligned} \upsilon_{\delta_{eq}} &= \dot{\phi}_q - a\left(\theta - f\right) - k_{z_q} z_q \text{ and} \\ \upsilon_{\delta_r} &= \dot{\phi}_r - b\left(\psi - g\right) - k_{z_r} z_r \end{aligned} \tag{19}$$

with $k_{z_q}, k_{z_r} \in \Re^+$, yields

$$\dot{V}_2 = \dot{V}_1 - k_{z_q} z_q^2 - k_{z_r} z_r^2 \leq 0.$$

From Barbalat's lemma, it can be concluded that $l_{\mathbf{N}}$, $l_{\mathbf{B}}$, θ and ψ converge to zero. Thus, the following theorem holds.

Theorem 2 *With the signals (19), the system (8)-(9),(14)-(15) asymptotically converges to the origin.*

5 Zero dynamics analysis

In the closed-loop system (1)-(5), (7)-(12), (19), the distance and angular errors are controlled and asymptotically convergent responses for $l_{\mathbf{N}}$, $l_{\mathbf{B}}$, θ and ψ are obtained. Furthermore, from equation (7), and since θ, ψ, and $l_{\mathbf{N}}$ tend to zero, $\dot{s} \to V_t$ reflecting the fact that, once the vehicle is on the path, the total velocity is tangent to trajectory. It remains to show that ϕ, p, α, and β are bounded. This is equivalent to proving boundedness of the zero dynamics of the vehicle. Due to the complexity of the equations, the analysis will be done only for the cases where the vehicle motion is confined to the horizontal and vertical planes. The analysis of the complete zero dynamics is still an open problem.

When the vehicle is restricted to navigate in the horizontal plane, the state variables are s, $l_{\mathbf{N}}$, ψ, β, and r (the other variables are set to zero). The zero dynamics are thus obtained from the $\dot{\beta}$ equation. Since z_r tends to zero, $\upsilon_r \to \phi_r$; (16) and the fact that $l_{\mathbf{N}}$ and ψ converge to zero shows that $\upsilon_r \to k\dot{s}$. Now, using equations (13) and (2), yields

$$\dot{\beta} = \frac{V_t}{L}\frac{Y_v}{Y_r}\beta + kV_t - \frac{2kmV_t\cos\beta}{\rho L^3 Y_r}$$

where the last two terms are bounded. By resorting to the comparison lemma (Khalil, 1996), β is bounded as long as $\frac{Y_v}{Y_r} < 0$.

In the vertical plane, the state variables are s, $l_{\mathbf{B}}$, θ, α, and q, and the zero dynamics are obtained from the $\dot{\alpha}$ equation. In this case the model should be slightly modified to accommodate for the necessary change of the reference path parameterization. Now, the path's curvature should be seen as a rotation about the y_{SF} axis. The details are omitted here, but it can be proven (as for the horizontal plane) that the zero dynamics reduces to

$$\dot{\alpha} = -\frac{V_t}{L}\frac{Z_w}{Z_q}\alpha - kV_t - \frac{2kmV_t\cos\alpha}{\rho L^3 Z_q}.$$

Again using the comparison lemma, $\dot{\alpha}$ remains bounded if $\frac{Z_w}{Z_q} > 0$.

It is interesting to point out that the conditions $\frac{Y_v}{Y_r} < 0$ and $\frac{Z_w}{Z_q} > 0$ require that the vehicle be stern dominant both in the lateral and vertical planes. For a definition of bow and stern dominant vehicles, see (Lewis, 1989, Chapter 9, Section 4.2).

6 Simulation results

The control law proposed was tested in simulation for a straight line and a helix. The controller gains were set to $a = b = 1$, $k_\theta = k_\psi = 10$, $k_f = k_g = 0.5$, $k_{z_q} = k_{z_r} = 0.01$, $\theta_d = 30°$, and $\psi_d = 45°$. The vehicle's forward speed was set to $1ms^{-1}$. Figure 2 shows that the vehicle approaches the straight line with the prescribed attitude relative to the path. Figure 3 depicts the vehicle trajectory and Figure 4 represents the

actuator signals, i. e., the stern and bow planes and rudder deflections, when the vehicle is following a helix.

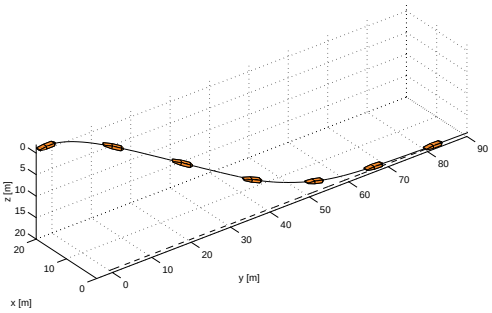

Figure 2: Vehicle following a straight line.

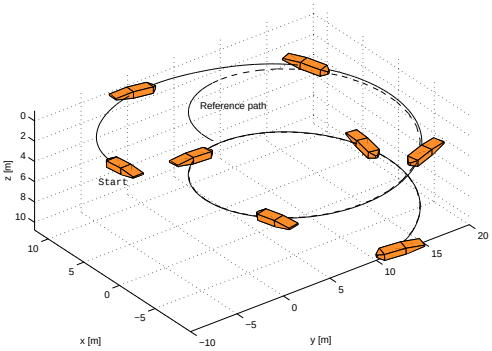

Figure 3: Vehicle following a helix.

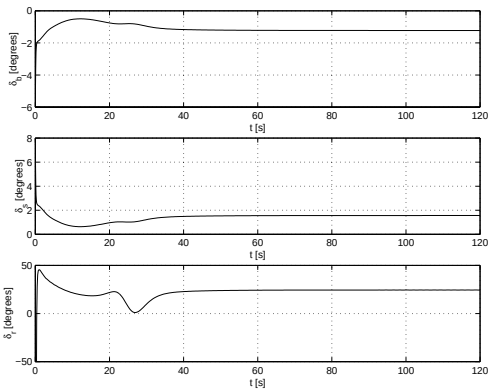

Figure 4: Actuator signals when following a helix: control surface deflections.

7 Conclusions and directions for future work

The paper described a new methodology for the design of path following systems for autonomous underwater vehicles in three dimensional space. The design builds on Lyapunov theory and resorts to backstepping techniques. Formal proofs are available that guarantee convergence of the vehicle to a desired path in the presence of vehicle dynamics. Further work is required to make the control laws robust in the presence of parametric uncertainty, include saturations in the actuator signals, and reject constant perturbations, namely ocean currents. See (Encarnação and Pascoal, 2000) for a solution to this problem.

References

Aamo, O. M., M. Arcak, T. I. Fossen and P. V. Kokotović (2000). Global output-tracking control of a class of Euler-Lagrange systems. In: *Proceedings of CDC'2000*. Sydney, Australia.

Craig, J. (1986). *Introduction to Robotics Mechanics and Control*. Addison-Wesley. New York.

Encarnação, P., A. Pascoal and M. Arcak (2000). Path following for marine vehicles in the presence of unknown currents. In: *Proceedings of SYROCO'2000, 6th IFAC Symposium on Robot Control*. Vienna, Austria.

Encarnação, P. and A. Pascoal (2000). Path following for autonomous underwater vehicles in the presence of unknown oean currents. Technical report. Instituto Superior Técnico. Lisbon, Portugal.

Fossen, T. I. (1994). *Guidance and Control of Ocean Vehicles*. John Wiley & Sons. Chichester, England.

Fossen, T. I. and S. Berge (1997). Nonlinear vectorial backstepping design for global exponential tracking of marine vessels in the presence of actuator dynamics. In: *Proceedings of CDC'97, IEEE Conference on Decission and Control*. San Diego, CA, USA. pp. 4237–4242.

Fryxell, D. J. (1994). Modeling, identification, guidance, and control of an autonomous underwater vehicle. Master's thesis. Department of Electrical Engineering, Instituto Superior Técnico. Lisboa, Portugal.

Fryxell, D., P. Oliveira, A. Pascoal, C. Silvestre and I. Kaminer (1996). Navigation, guidance, and control of AUVs: An application to the MARIUS vehicle. *IFAC Journal of Control Engineering Practice* **4**(3), 401–409.

Isidori, A. (1989). *Nonlinear Control Systems*. Springer-Verlag. Berlin.

Kaminer, I., A. Pascoal, E. Hallberg and C. Silvestre (1998). Trajectory tracking for autonomous vehicles: An integrated approach to guidance and control. *Journal of Guidance, Control, and Dynamic Systems* **21**(1), 29–38.

Khalil, H. K. (1996). *Nonlinear Systems*. Second ed. Prentice-Hall. New Jersey.

Krstić, M., I. Kanellakopoulos and P. V. Kokotović (1995). *Nonlinear and Adaptive Control Design*. John Wiley & Sons, Inc. New York.

Lewis, E. V., (Ed.) (1989). *Principles of Naval Architecture*. Second Revision. Vol. III. SNAME. Jersey City, NJ.

Micaelli, A. and C. Samson (1993). Trajectory tracking for unicycle-type and two-steering-wheels mobile robots. Technical Report 2097. INRIA. Sophia-Antipolis, France.

Pascoal, A. *et al.* (2000). Robotic ocean vehicles for marine science applications: the european ASIMOV project. In: *Proceedings of OCEANS'2000 MTS/IEEE*. Rhode Island, Providence, USA.

Samson, C. (1992). Path following and time-varying feedback stabilization of a wheeled mobile robot. In: *Proceedings of ICARV*. pp. RO–13.1.

Silvestre, C. and A. Pascoal (1997). Control of an AUV in the vertical and horizontal planes: System design and tests at sea. *Transactions of the Institute of Measurement and Control* **19**(3), 126–138.